Computed tomography 3-D imaging of the metal deformation flow path in friction stir welding

Judy Schneider
Department of Mechanical Engineering
Mississippi State University
Mississippi State, MS 39762

Ronald Beshears
ED32 Marshall Space Flight Center
Non-Destructive Evaluation Team
Huntsville, Alabama 35812

Arthur C. Nunes, Jr.
ED33 Marshall Space Flight Center
Materials Processes & Manufacturing Dept.
Huntsville, Alabama 35812

Abstract

In friction stir welding (FSW), a rotating threaded pin tool is inserted into a weld seam and literally stirs the edges of the seam together. To determine optimal processing parameters for producing a defect free weld, a better understanding of the resulting metal deformation flow path is required. Marker studies are the principal method of studying the metal deformation flow path around the FSW pin tool. In our study, we have used computed tomography (CT) scans to reveal the flow pattern of a lead wire embedded in a FSW weld seam. At the welding temperature of aluminum, the lead becomes molten and is carried with the macro-flow of the weld metal. By using CT images, a 3-dimensional (3D) image of the lead flow pattern can be reconstructed. CT imaging was found to be a convenient and comprehensive way of collecting and displaying tracer data. It marks an advance over previous more tedious and ambiguous radiographic/metallographic data collection methods.

I Introduction

Figure 1 illustrates the configuration of a FSW tool relative to a panel being joined. A threaded pin tool is inserted into the metal, rotated at a fixed rate, and traverses the length of the butt weld. The tool is tilted at a slight lead angle and a plunge force constrains the metal between the tool shoulder and a backing anvil.

An overview of a FSW butt joint is presented in Figure 2 showing the 3 images that will be discussed. A striking feature of a FSW is the banding observed in light microscopy images of the microstructure. Distinct banding in the center nugget region can be observed in the transverse, lateral, and normal views shown in Figure 3-5, respectively, suggesting a 3D flow path. The spacing of the banding in Figure 4 and 5 correlates with the distance traversed during a single rotation of the tool. Figure 6 provides an illustration of how periodic shedding occurs from the rear of the tool in the wake of the weld and is believed to result in the ring pattern. Although there have been numerous manuscripts discussing the origin of the banding, the general conclusion presented in the literature is that its presence does not affect the quality of the weld nugget [1-3].

Marker studies have revealed most of what is known about friction stir weld flow patterns [3-8]. Early studies of welds in dissimilar metals reported a chaotic pattern of the metal flow [3-4]. Colligan's [5] research with 0.015 in steel shot seeded in a butt weld joint showed an orderly movement of material in response to the weld tool movement. Studies by Seidel and Reynolds [6] with marker inserts defined differences in the advancing vs. retreating side of the weld. Although beneficial in helping to understand the material flow during FSW, marker studies are tedious to execute and the results are difficult to interpret. In this study, computed tomography is used to reconstruct 3-dimension (3D) images of a lead wire that was embedded in the weld seam prior to a butt weld.

II Background - proposed model of metal flow in FSW

Interpretation of the metal flow in a FSW is hampered by the lack of a model to assist in the determination of optimized parameters. Thus, although various marker studies have been reported, separation of the optimized flow from flow anomalies is difficult.

As illustrated in Figure 1, the friction stir welding tool presses the weld metal down in the vicinity of the pin with the shoulder. This requires a downward "plunge force" on the tool sufficient to resist the pressure of the weld metal and maintain the tool in place. In normal operation the configuration of the pin tool contour is designed to seize the metal and usually consists of a coarsely threaded pin tool. This induces a plastic flow field in the weld metal as illustrated in Figure 7a.

If the plunge force were insufficient, the plastic slip zone would not extend all the way to the edge of the shoulder as illustrated in Figure 7b. This would result in some frictional slippage at the shoulder. To avoid this occurrence, sufficient, or optimized plunge forces would be required to ensure the shearing or plastic flow occurred in the weld metal. There could also be instances where the process may alternate between plastic flow and frictional slippage, or a stick-slip mode of operation.

III Procedure

The material used in this study was 2195-T81 Al-Li-Cu alloy. Full penetration welds were made on an 0.323 in thick plate with a pin tool 0.312 in long. The pin diameter was 0.50 in and the smooth shoulder diameter was 1.20 in. The tool was operated with a back tilt or "lead angle" of 2.5°. A left-handed 0.050 in pitch threaded pin was used at spindle speed of 200 rpm and a traverse speed of 6 in/min) along the rolling direction of the plate.

The first weld panels were made with a 0.0025 in diameter tungsten wire embedded in the weld seam. The wire was placed in the center of the butt joint as illustrated in Figure 8 and the weld made with the tool transversing the butt joint. The weld was made in position control mode with an average plunge force of 8,600 lbs. Final wire placement was documented in this sample using x-ray radiography prior to serial sectioning of transverse and longtitutional metallographic sections. Spacing of the wire segments determined from the x-ray radiographs was used to guide the material removal in serial sectioning.

The x-ray radiographs taken of the weld seam in both lateral and normal orientations are shown in Figure 9a and b, respectively. Sections of the weld panel with the tungsten wire were removed, mounted, and polished for metallographic analysis. Keller's reagent was used to etch the samples for metallographic contrast. The wire location was recorded by use of optical microscopy. The sample was serially sectioning by polishing the surface in 0.02 to 0.028 in increments as determined from the x-ray radiographs. Optical micrographs of the lateral section of this weld are shown in Figure 10.

A second set of weld panels was made with a tungsten wire, 0.001 in diameter, embedded along a scribe mark in the butt joint, 0.05 in from the shoulder surface. Two separate welds were made with the pin tool offset to either side of the butt joint as shown in the normal x-ray radiographs in Figure 11a and b. Both welds were made in position control mode with an average plunge force of 10,200 lbs.

A third set of weld panels was made with a lead wire, 0.010 in diameter, embedded along a scribe mark in the butt joint, 0.05 in from the shoulder surface. The pin tool was offset to place the lead wire on the left, or advancing side of the weld as shown in Figure 11 and 12. Although not measured in this experiment, reported temperatures during FSW of aluminum range from 450 to 480 °C [1, 7, 8]. This is well above the reported melting temperature for lead of 328 °C. The weld was made in position control mode with an average plunge force of 10,600 lbs.

Unique markings were noted in a 4 in section of the x-ray radiograph normal to the FSW joint with the lead wire embedded as illustrated in Figure 12c. This portion was removed and imaged using FlashCT® computed tomography (CT) from HYTEC Inc. The FlashCT system, illustrated in Figure 13, incorporates a 420 kV Pantak x-ray tube and Varian 2520 amorphous silicon flat-panel detector. Raw data acquired at a 5M pixel resolution is converted to 3D form with fan, parallel and cone beam reconstruction algorithms. Slice animation and interrogation are coupled with the volume rendering to provide visual access to the interior of the FSW sample.

IV Results

Although some scatter was observed in the X-ray radiographs of the tungsten wire samples embedded in the center of the FSW joint, the wire segments were uniform in length and tended to remain in the center of the weld joint. Serial sectioning of the 0.025 in wire diameter sample allowed comparison of the wire segments placement with respect to the banding pattern. Sectioning of the lateral section showed an irregularity in the wire segment placement. If each segment of wire is considered to represent the flow in one weld tool rotation, variation in the shedding pattern in the tool wake was noted as shown in Figure 10.

X-ray radiographs of the weld panel with the lead wire embedded in the weld joint at 0.05 in below the surface, are shown in Figure 12. Three different images were observed and are shown. Although resolution of the lead wire was difficult to observe in the first 11.5 in of the weld, some traces could be observed corresponding to the 1.2 in shoulder diameter (Figure 12a). A very pronounced tracing was observed in a 3 in segment at a weld distance of 11.5 to 14.5 in (Figure 12c) and again in the final 0.5 in (Figure 12b) of the weld travel prior to termination. The tracings in Figure 12b and c correspond to the pin diameter and appeared to be bundled groups of streaks with spacings on the order of multiples of 0.03 in.

To further explore the features in the weld segment from 11.5 to 14.5 in, the section shown in Figure 14 was removed and inspected using CT imaging. The aluminum metal was subtracted from the images shown to allow examination of the lead traces. The specimen was scanned in two orientations as illustrated in Figure 15 with the red, green, and blue planes cutting thru the

specimen. This data was reconstructured into a 3-D image that can be rotated to observe the banded patterns of the lead. Figure 16 shows one such isometric view of the lead wire remnants.

IV Discussion

In the weld with the lead wire tracer, it is assumed that the lead, which melts at the anticipated welding temperatures, is carried with the macro-flow of the weld metal and does not produce its own artificial flow patterns at the macro-scale observations of the radiographs. The dispersion of the lead tracer patterns resembles the tracer patterns noted in previous research by Colligan [5]. An explanation for the origin of these tracer patterns will be discussed in terms of macro-flow patterns around the tool and will be assumed to be representative of actual residual flow patterns in the weld metal.

The complex flow field around a FSW tool can be decomposed into three simpler component fields illustrated in Figure 17. The component fields, and their composite, are incompressible flows.

The axial rotation of the tool clearly induces an axial, or rigid body rotation in the surrounding weld metal. But how does the induced rotation vary with radius? Figure 5 exhibits a plan section of a friction stir weld. The section is taken at mid-plate level, i.e. about halfway through the plate thickness. A very sharp division between recrystallized metal adjacent to the pin-tool and parent metal is apparent. The sharply defined circular boundary between the recrystallized metal and the

parent metal suggests a shear circle discontinuity around the tool much like the shear plane encountered ahead of a metal-cutting tool. The threaded surface of the pin is taken as sufficient to induce seizure at the pin/weld metal surface and to rotate the metal inside the shear surface with essentially the same rotational speed as the pin. Recent studies [9] suggest that a relatively slow rotation induced outside the shear surface has a significant effect on the residual weld structure and needs to be taken into account. To simplify the discussion, the secondary rotation will be combined and treated the same as the primary rotation with a secondary shear surface with a much smaller velocity discontinuity at its boundary. Only the secondary rotation is believed to be operative in causing the phenomena discussed.

Hence the first of the flow components (Figure 17a) is a rigid body rotation separated from the rest of the weld metal by a cylindrical shearing surface, a surface of velocity discontinuity. The rigid body rotation represents a plug of weld metal surrounding and rotating with (but not necessarily with the same rotational speed as) the FSW tool. The boundary of the primary circulation tends to hug the tool toward the bottom of the pin with a slight increase in thickness on the retreating side to accommodate metal transfer to the rear of the pin as the pin moves. The outer, secondary circulation does likewise. The shearing cylinder bounding either primary or secondary rotation expands toward the tool shoulder, either all the way to the edge of the shoulder or to the radius at which plastic shear gives way to frictional slip on the outer regions of the shoulder.

The second flow component is a homogeneous, constant velocity flow field representing the tool traverse velocity. When the first and second components are combined, a rough representation of

the flow around a FSW tool is obtained: a swirling motion translating through the weld metal. This representation can be visualized from a coordinate system fixed either on the tool or on the weld metal. Seen from the tool a metal element in the combined flow field: 1. approaches the tool at the weld traverse speed, 2. enters the rotating plug at the shear surface and is whisked rapidly around the tool at the rotational field surface speed in a slightly laterally offset circular arc, and 3. exits at the rear of the tool to move progressively away at the tool traverse speed. Seen from the weld metal the metal element: 1. remains motionless until contacted by the shear surface of the rotational field, 2. is engulfed by the rotational field and covered by subsequently engulfed elements as it is whisked rapidly around the tool, and 3. is gradually uncovered as the elements between it and the shearing surface are abandoned behind the tool and is finally abandoned itself as the rotational field moves on. We have called this mechanism the "wiping metal transfer mechanism" [10]. During the time the element resides in the rotating field it is not deformed. Deformation only occurs during the crossing of the shear surface.

The first two flow components are limited to motion only in the plane perpendicular to the tool axis, but tracer experiments [5] have shown that axial motion also takes place. A third flow component is incorporated into a FSW model to represent axial motion effects. Axial motion is induced by threads on the pin and/or scrolled ribbing on the tool shoulder and is reversed if the direction of the threads/ribs or the direction of tool rotation is reversed. In normal operation the axial flow is downward, i.e. away from the shoulder, close to the tool. The FSW anvil blocks the downward flow, so what goes down at the pin must come back up at a greater radius. The tool shoulder blocks the upward flow, so that the flow is diverted again inwards to flow back down the tool in a circular motion. The flow takes the form of a circulation in a plane incorporating

the shear surface axis as illustrated in Figure 7. There is such a circulation within any plane incorporating the shear surface axis. The successive circulations in a plane rotated about the shear surface axis generate a vortex ring, which may be visualized like a smoke ring, another form of ring vortex, about the FSW pin (Figure 17c).

The third flow component, then, is a ring vortex flow field encircling the tool and bringing metal up on the outside, in at the shoulder, down on the inside, and out again on the lower regions of the pin. The ring vortex velocity field is relatively slow and continuous. Like the other two components it conserves volume, so that the combination of all three-velocity fields also conserves volume.

The strictly axial velocity components of the ring vortex field don't interact with the first two components, but the radial components do. Their interaction explains lateral shifts in tracers. Because of the symmetry of the engulfment and abandonment processes with the first two components only, an element of weld metal or tracer engulfed by the shear surface at a given distance from the line of motion of the tool is abandoned at the identical distance. Seen from the tool, a tracer approaches the tool and departs from the tool along the same line. With a radial flow component due to the ring vortex the weld metal or tracer element is retained longer (inward component) or expelled earlier (outward component). Longer retention shifts the expulsion point toward the advancing side of the weld.

The above model explains many of the features observed in earlier tracer experiments [5, 9], but it explains neither all features nor certain particularly pronounced features of the present lead

wire tracer study (Figures 12, 15, 16). The expulsion points of the tracer are dispersed into a smear in the lead wire experiment. Shot tracer expulsion points are also widely laterally dispersed [5, 9] close to the tool shoulder (in a position not unlike that of the lead wire).

Oscillation of the shear surface radius would result in the observed dispersions! An increasing radius retains the weld metal or tracer element longer in the rotational field for a shift to the advancing side. A decreasing radius results in an earlier expulsion for a shift to the retreating side. Continuous change results in a continuous dispersion of expulsion points. The decreasing radius phase of the oscillation explains the observation of tracer on the retreating side of the wire line of entry. The anticipated inward velocity component of the ring vortex close to the shoulder would only explain advancing side displacements.

The irregular spacing of the lead tracer arcs behind the tool shown in Figure 12b and c requires that an irregular mechanism be postulated for it. These markings do not appear in the initial 11.5 inches of weld shown in Figure 12a, presumably because the periodic spacing of shear radius oscillations is so small as to disperse the lead along the weld to such an extent that it becomes difficult to see. The wide irregular spacings of Figure 12 b and c are presumably associated with the somewhat hotter weld as contrasted with a cooler initial transient weld phase. Sporadic sticking and slipping at the edge of the shoulder, as illustrated in Figure 7, provides a possible explanation.

Figure 7 illustrates how an intermittent seizure and release at the outer surface of the tool shoulder can produce changes in the shear surface radius, which, in turn, can cause sporadic

losses of contact with the tracer and associated gaps in the trace pattern left behind the tool. During periods of contact between shear surface and wire a trace is left behind the tool. If the radius varies continually during contact, the trace will be dispersed. Figure 12 seems to reveal a double periodicity, a regular fluctuation apparently at the same frequency as the tool rotation double periodicity, a regular fluctuation apparently at the same frequency as the tool rotation and a slower irregular fluctuation modulating the more rapid fluctuation. The slow irregular fluctuation is responsible for the pronounced traces seen in Figures 12, 15, and 16. Whereas the regular fluctuations occur with the tool rotation frequency of 200 per minute, the slower fluctuations, spaced an order of magnitude more widely occur at a frequency on the order of 20 per minute. Incorporating high speed torque measurements during the FSW process would be an effective means of assessing and verifying instances of surface seizure and slipping.

V Summary

Conventional radiography and 3-D CT imaging were used to study the trace of a lead wire left subjected to the flow field of a FSW tool. The tool approached the wire on its advancing side 0.05 in below its shoulder. The trace pattern left behind comprised arc-shaped segments on the advancing side of the tool distributed with a double periodicity. A fine distribution at the period of tool rotation was modulated in amplitude with an irregular period roughly an order of magnitude longer. The irregular modulation was seen only after the weld had traveled a distance of 11.5 in.

From the dispersal of the wire into arcs and the gaps between the arcs it was inferred that the radial distribution of the rotational field around the tool oscillates. The proposed cause of the long period, irregular fluctuations in lead tracer amplitude is a sporadic seizure and release of metal contact at the edge of the FSW tool shoulder. Further studies are required to confirm this observation.

A particularly interesting implication of this interpretation is that the putative intermittent seizure and release of metal at the edge of the shoulder may have a significant effect upon the structure of the weld, and, although the presence of banding in the well-known onion-ring structure of the weld nugget has not been shown to affect the quality of the weld [1-3], it is conceivable that the structural changes may affect the weld integrity.

VI References

1. W. Tang, X. Guo, J.C. McClure, L.E. Murr, A.C. Nunes, Jr.: *J. Mat'l Process. & Mfgt. Sci.*, 1998, vol. 7, pp. 163-172.
2. A.F. Norman, I. Brough, P.B. Prangneil: *Mat'l Sci. Forum*, 2000, vol. 331-337, pp. 1713-1718.
3. Y. Li, L.E. Murr, J.C. McClure: *Scripta Mater.*, 1999, vol. 40, no. 9, pp. 1041-1046.
4. Y. Li, L.E. Murr, J.C. McClure: *Mat. Sci. & Engr.*, 1999, vol. A271, pp. 213-223.
5. K. Colligan: Welding Research Supplement, 1999, pp. 229s-237s.
6. T.U. Seidel, A.P. Reynolds: *Met. & Mat. Trans.*, 2001, vol. 32A, pp. 2879-2884.
7. L.E. Murr, G. Liu, J.C. McClure: *J. Mat. Sci.*, 1998, vol. 33, no. 25, pp. 1243-1251.
8. Y.S. Sato, M. Urata, H. Kokawa: *Metall. & Mat. Trans.*, 2002, vol. 33A, pp. 625-635.
9. J.A. Schneider: NASA-CR-2004/213285, 2004, pp. XXXIX 1-5.
10. A.C. Nunes, Jr: in *Automotive Alloys and Joining Aluminum*, eds, G. Kaufamann, J. Green, S. Das, TMS Warrendale, PA, 2001, pp. 235-248.

List of Figures

8. Configuration of the metal plates for the butt welds. Wire was placed in a scribed groove in the joint, prior to weld.

9. (a) X-ray radiograph of side (lateral) view of weld panel with 0.0025 in diameter wire and (b) X-ray radiograph of normal view of weld panel with 0.0025 in diameter wire.

10. (a) Lateral section of FSW exposing wire segments.
(b) Overlaying of 6 serial sections of the lateral view indicates wires are not directly related to one-to-one with the band spacing.

11. Tungsten wire (0.0254 mm dia.) inserted into weld seam at 1.27 mm (0.05 in) below shoulder. (a) Wire placed on advancing side of weld joint and (b) retreating side of weld joint.

12. Normal x-ray radiograph of weld panels with lead wire embedded in weld seam. The lead was resolved in arcs corresponding to the shoulder diameter in (a) and corresponding to the pin diameter in (b) and (c).

13. Configuration of the Hytec FlashCT System used to construct 3-D image of the lead wire trace.

14. A section (4.6 in) removed from the weld panel for CT scanning. Sample is 1.2 in wide x 4.6 in long x 0.32 in thick.

15. Scanning of slices in two orientations was able to be reconstructured to provide 3 planes of data in the FSW sample.

16. Isometric view of lead wire trace in FSW sample. Note the aluminum matrix has been subtracted from view.

17. Three incompressible flow fields of the friction stir weld: a) rigid body rotation, b) uniform translation, and c) ring vortex.

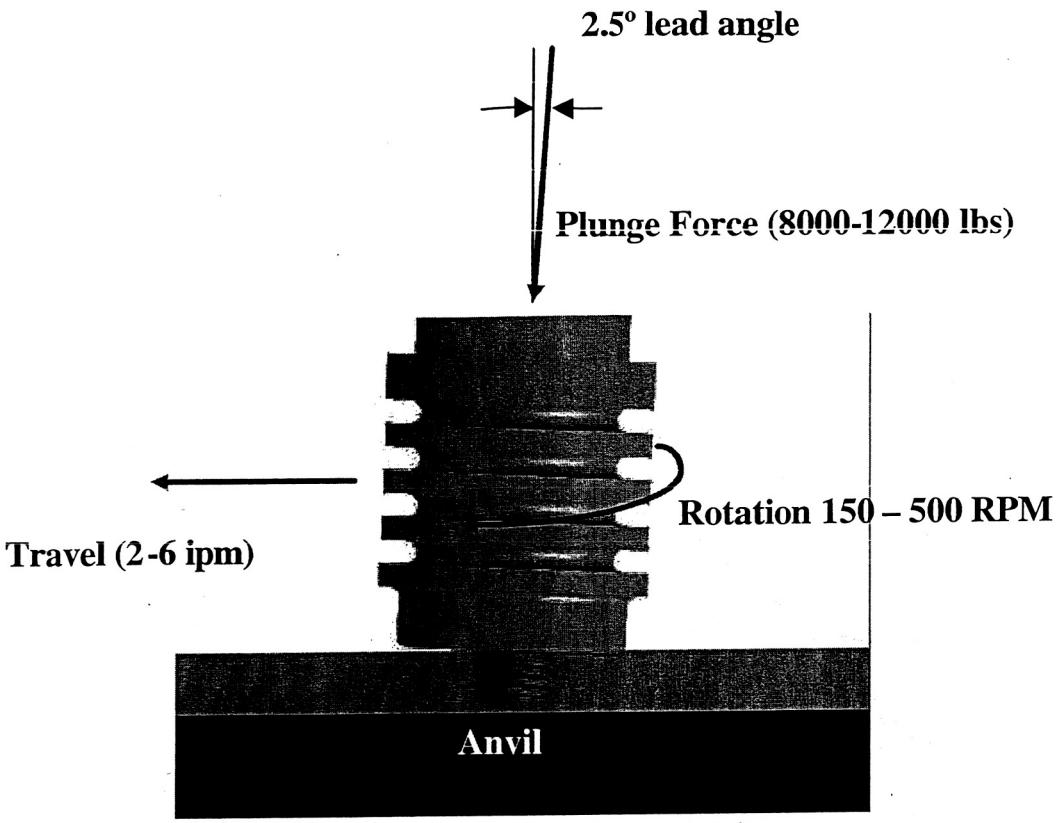

Figure 1. Terminology and typical weld parameter for FSW process.

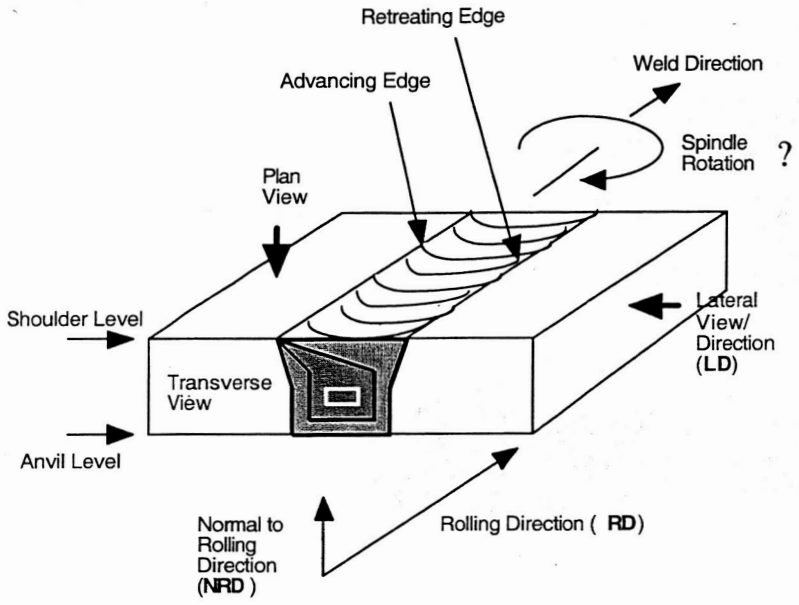

Figure 2. Nomenclature to be used for views (transverse, lateral, and plan), directions (lateral/LD, rolling/RD, normal to rolling/NRD), and plan view levels (shoulder, anvil) cited in this paper.

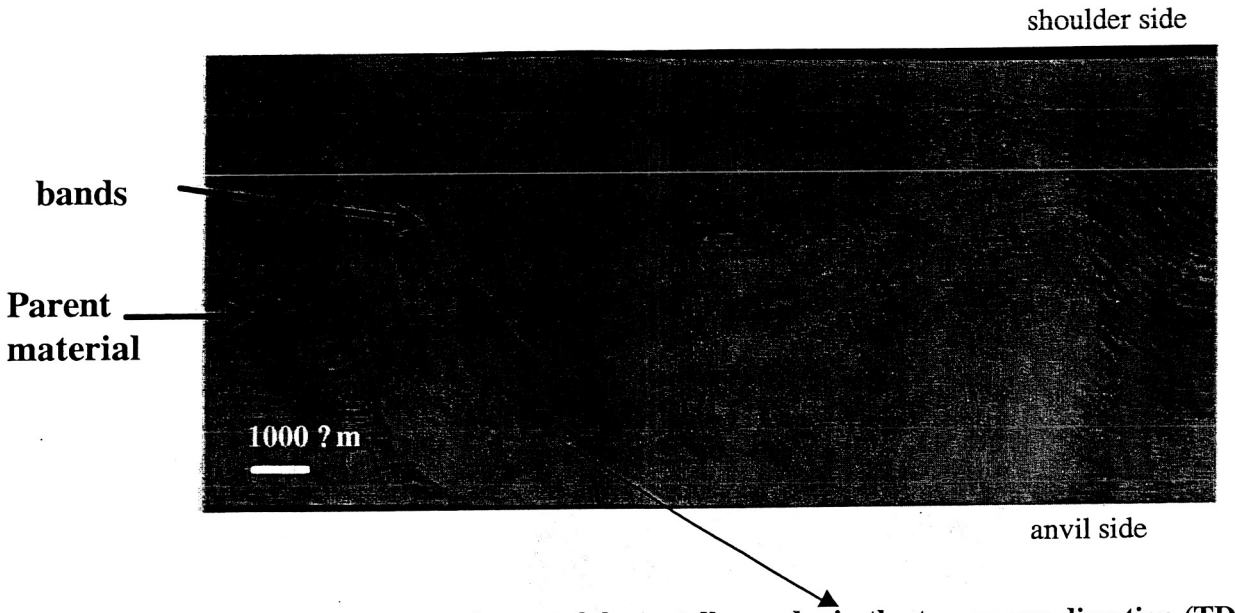

Figure 3. Light microscopy image of the metallography in the transverse direction (TD) of the FSW joint.

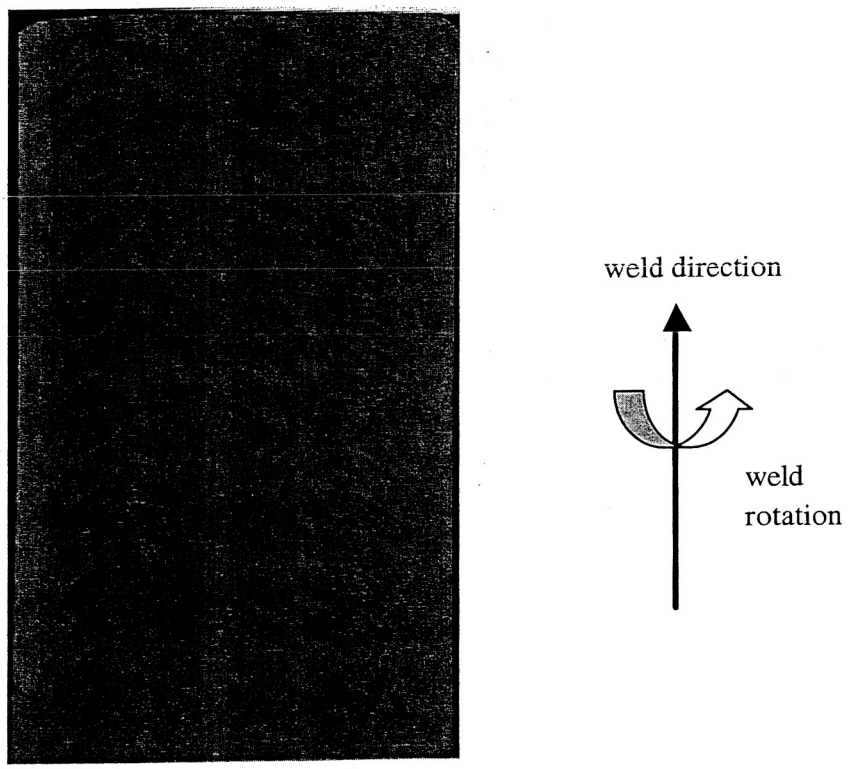

Figure 4. Light microscopy image of the metallography in the lateral direction (LD) of the FSW joint.

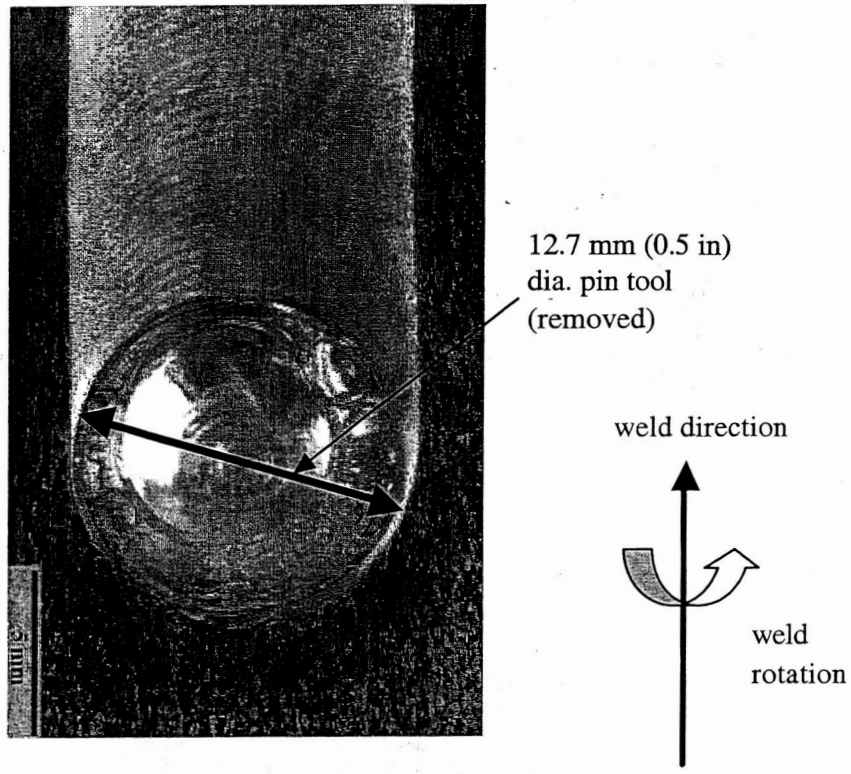

Figure 5. Light microscopy image of the metallography in the normal view of the FSW joint. The top material has been removed and the surface shown is at the center line of the plate thickness.

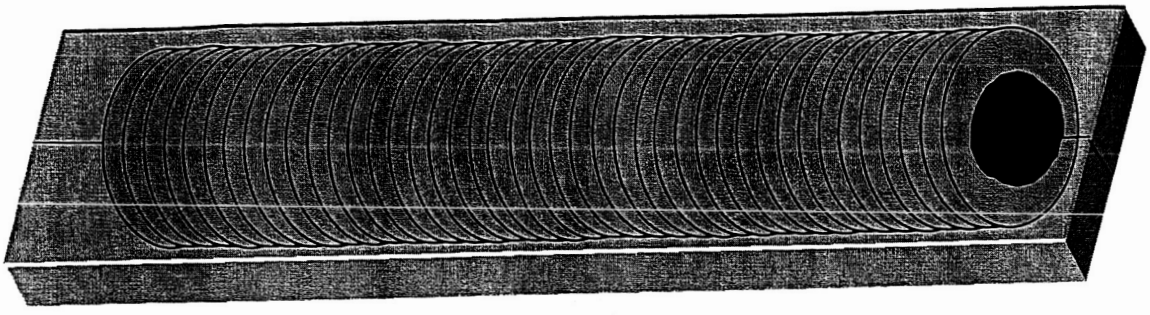

Normal view of FSW panel

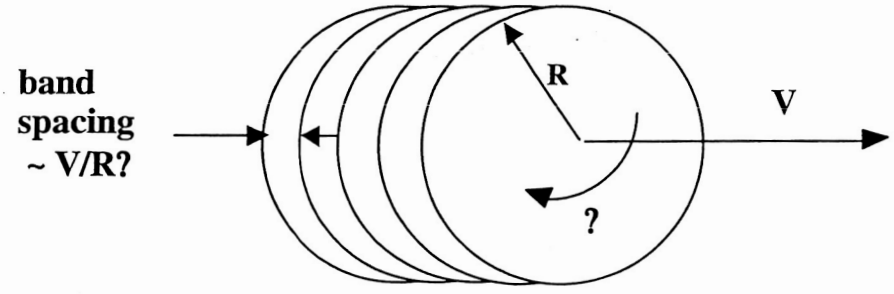

Figure 6. Spacing of the bands related to the translational rotation of the pin tool and weld travel speed.

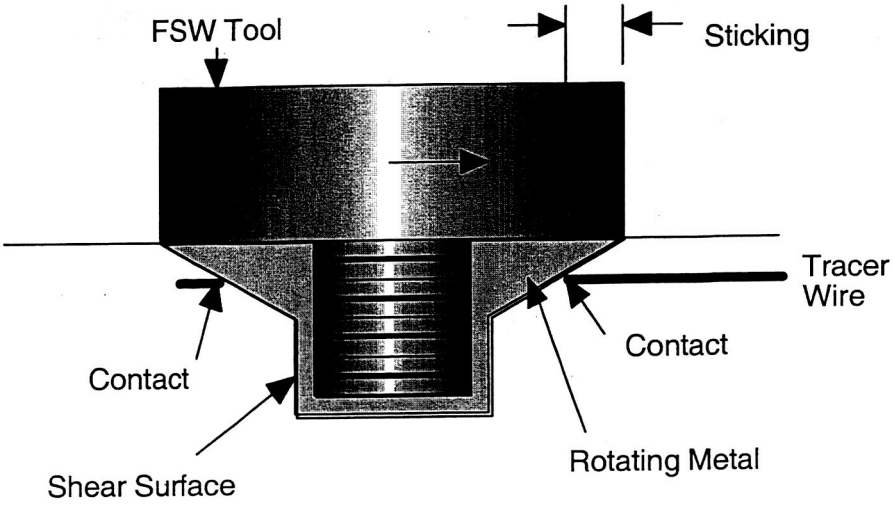

(a) plastic flow zone

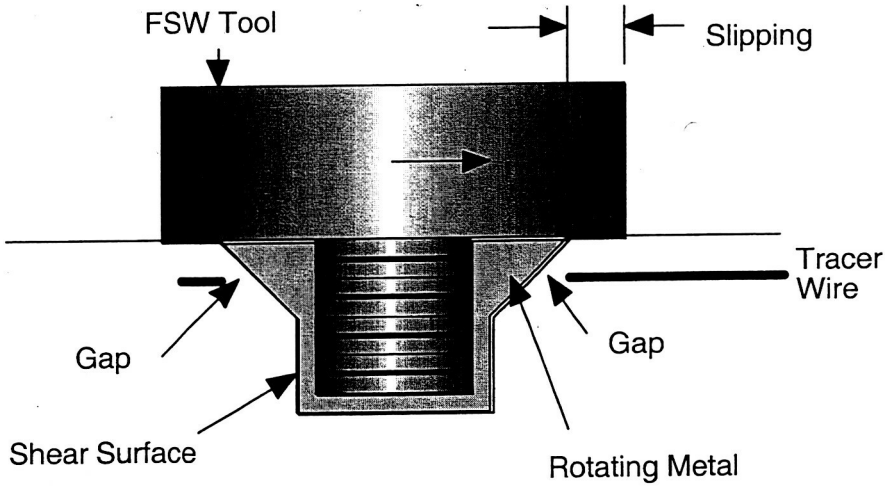

b) frictional slippage zone

Figure 7. Sporadic fluctuations in surface contact at edge of FSW tool shoulder can give rise to gaps in wire trace through variations in the radius of the shear surface.

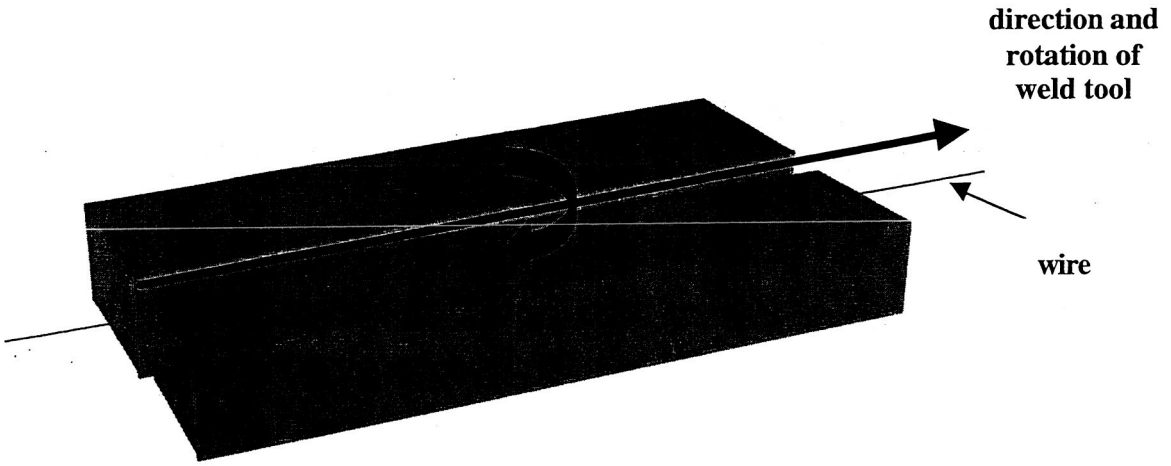

Figure 8. Configuration of the metal plates for the butt welds. Wire was placed in a scribed groove in the joint, prior to weld.

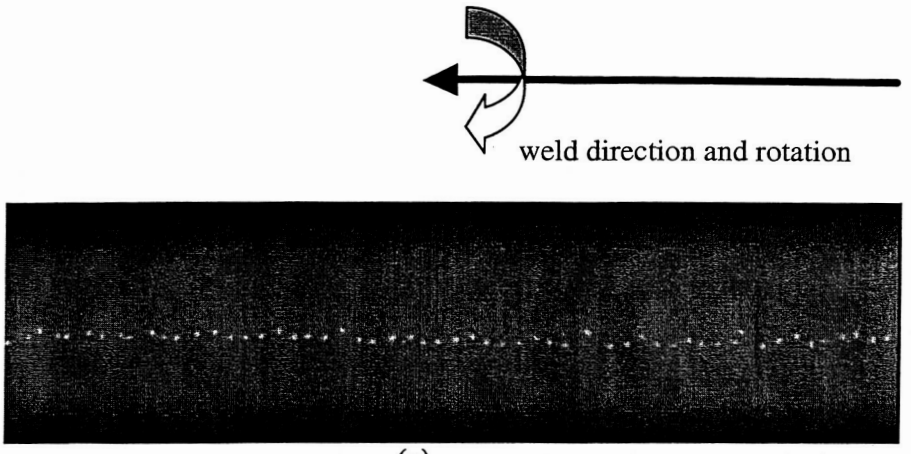

(a)

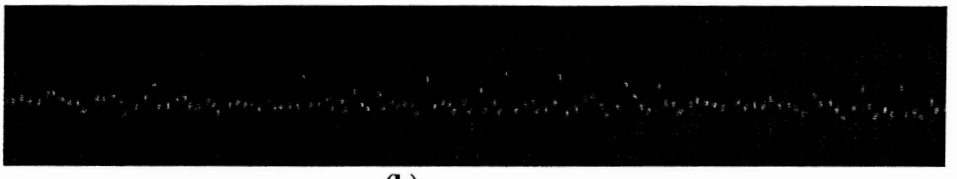

(b)

Figure 9. (a) X-ray radiograph of side (lateral) view of weld panel with 0.0025 in diameter wire and (b) X-ray radiograph of normal view of weld panel with 0.0025 in diameter wire.

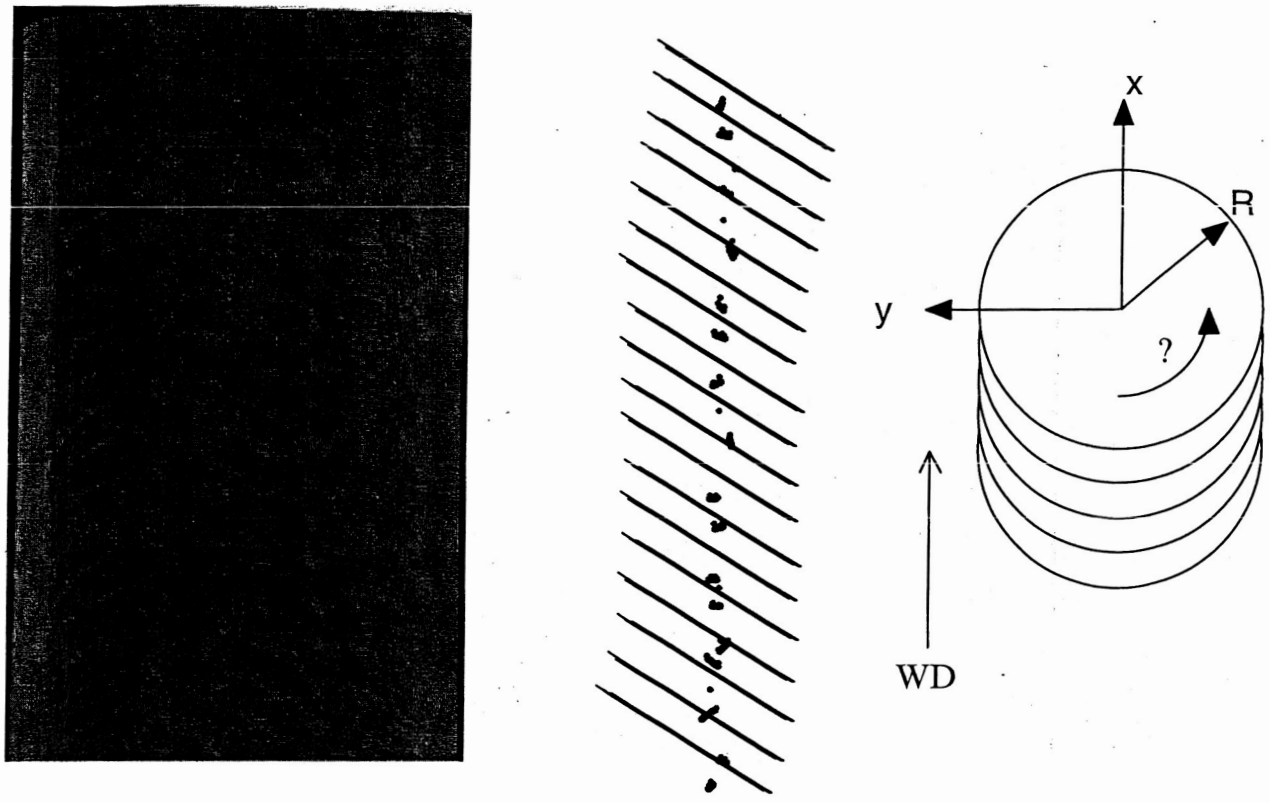

(a) (b)

Figure 10. (a) Lateral section of FSW exposing wire segments. (b) Overlaying of 6 serial sections of the lateral view indicates wires are not directly related to one-to-one with the band spacing.

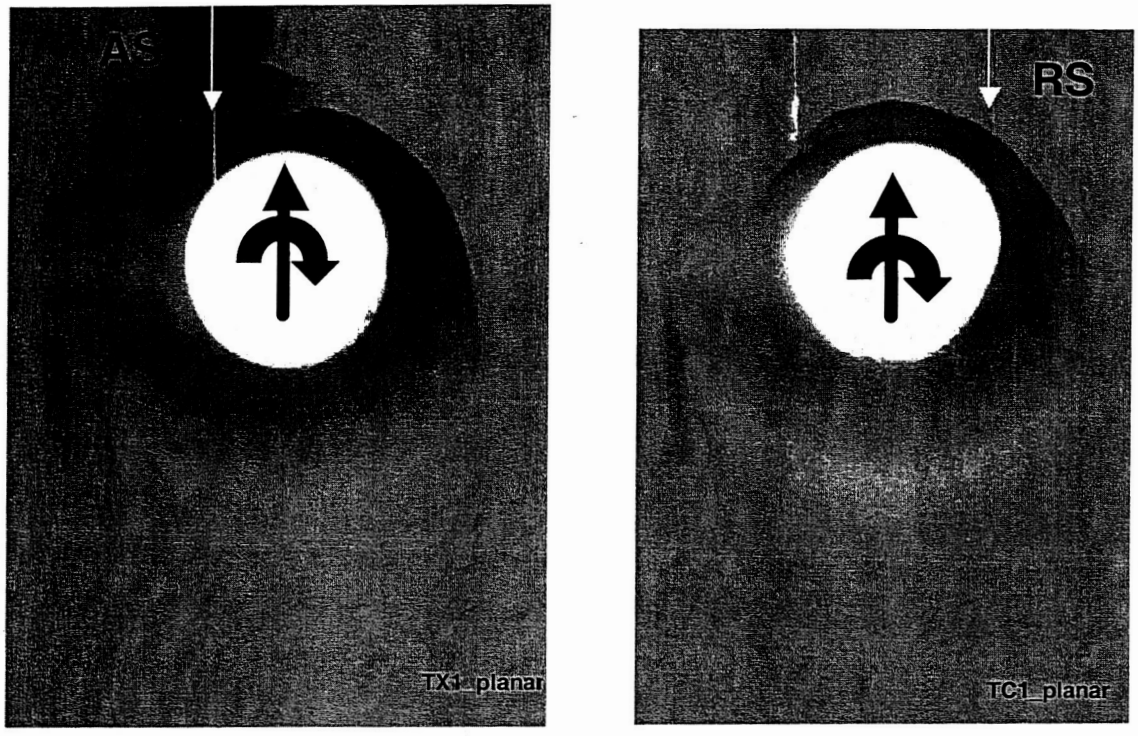

(a) (b)

Figure 11. Tungsten wire (0.0254 mm dia.) inserted into weld seam at 1.27 mm (0.05 in) below shoulder. Wire placed on (a) advancing side of weld joint and (b) retreating side of weld joint.

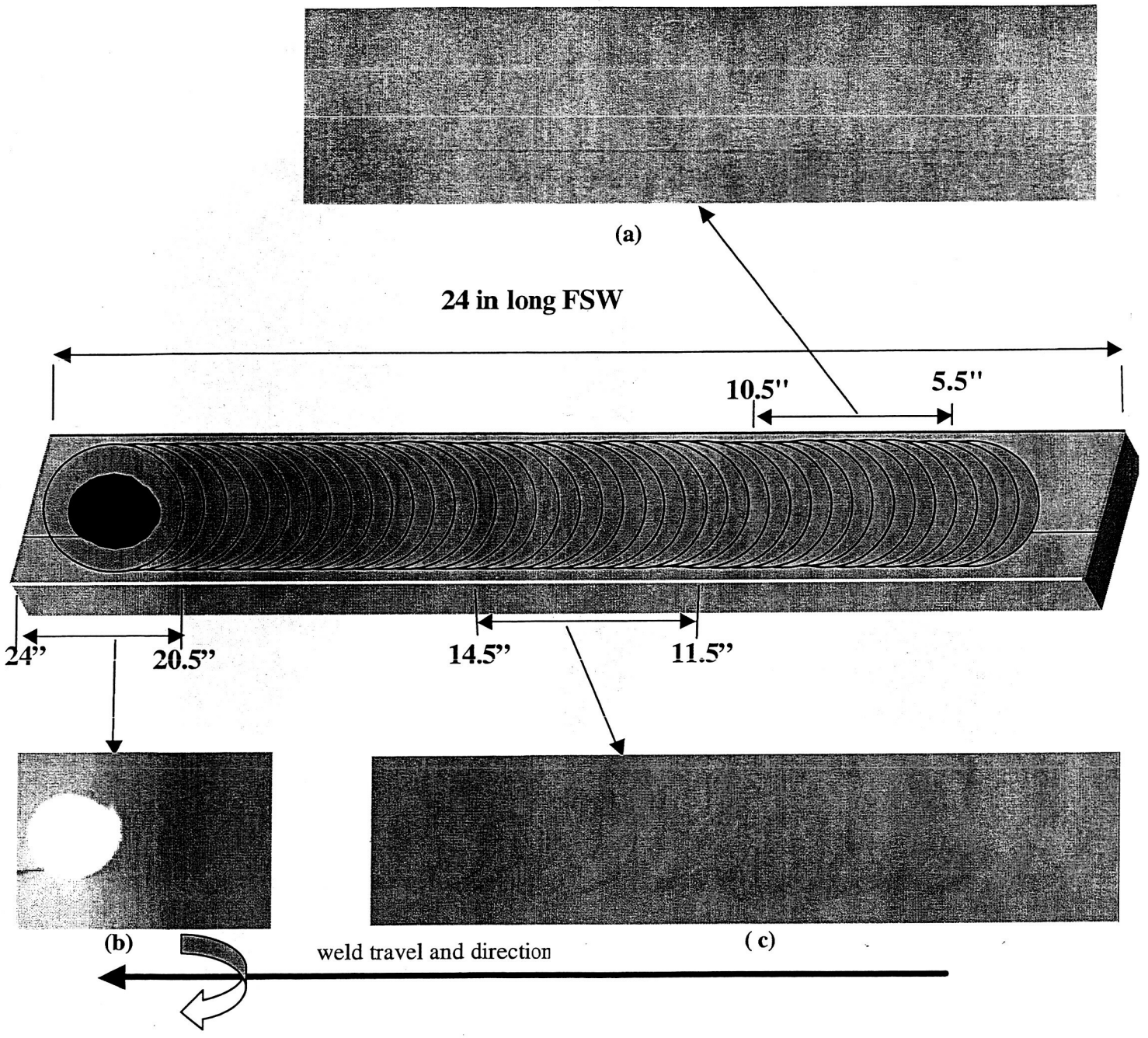

Figure 12. Normal x-ray radiograph of weld panels with lead wire embedded in weld seam. The lead was resolved in arcs corresponding to the shoulder diameter in (a) and corresponding to the pin diameter in (b) and (c).

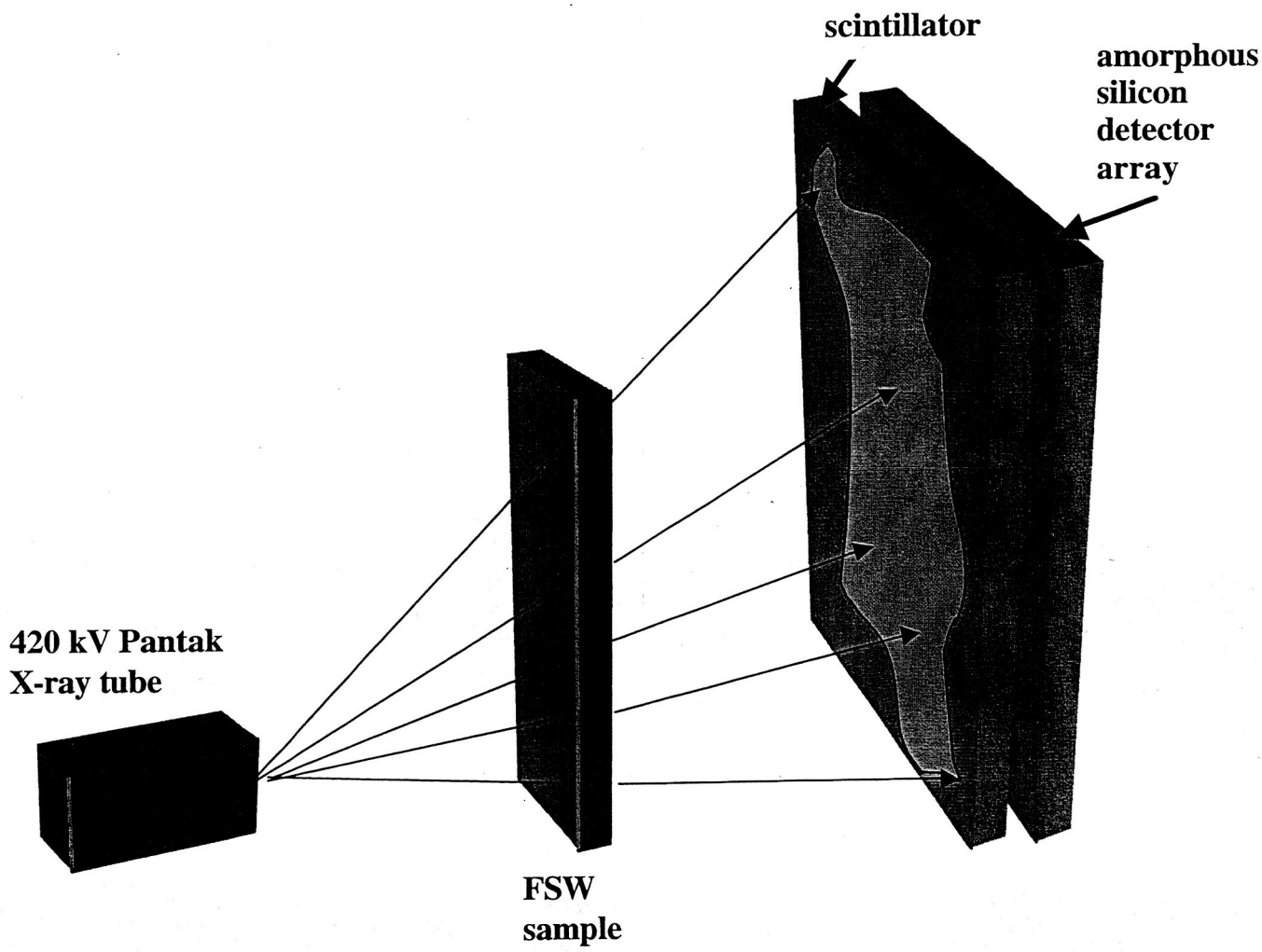

Figure 13. Configuration of the Hytec FlashCT System used to construct 3-D image of the lead wire trace.

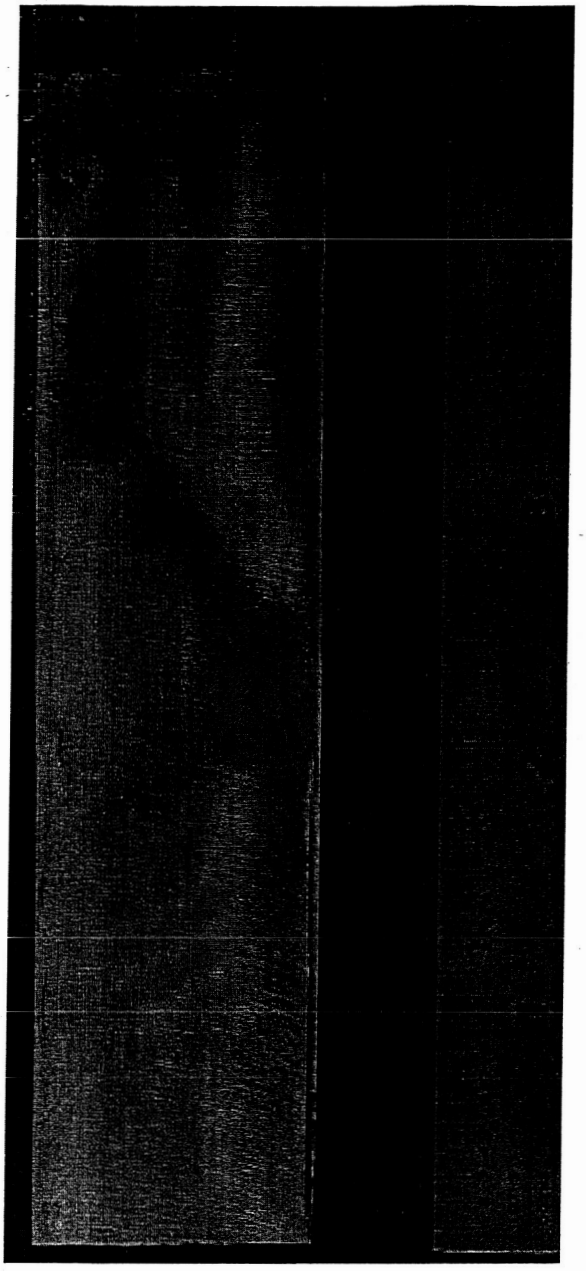

Figure 14. A section (4.6 in) removed from the weld panel for CT scanning. Sample is 1.2 in wide x 4.6 in long x 0.32 in thick.

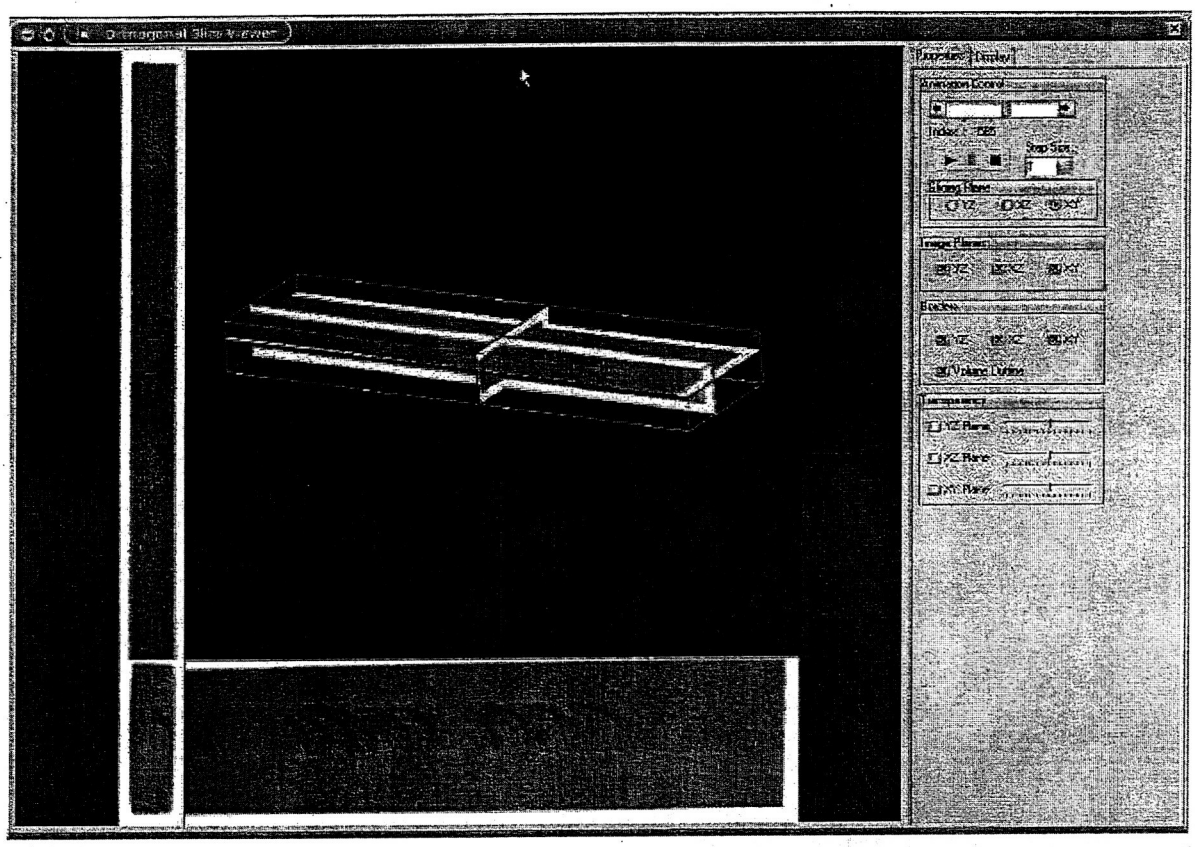

Figure 15. Scanning of slices in two orientations was able to be reconstructured to provide 3 planes of data in the FSW sample.

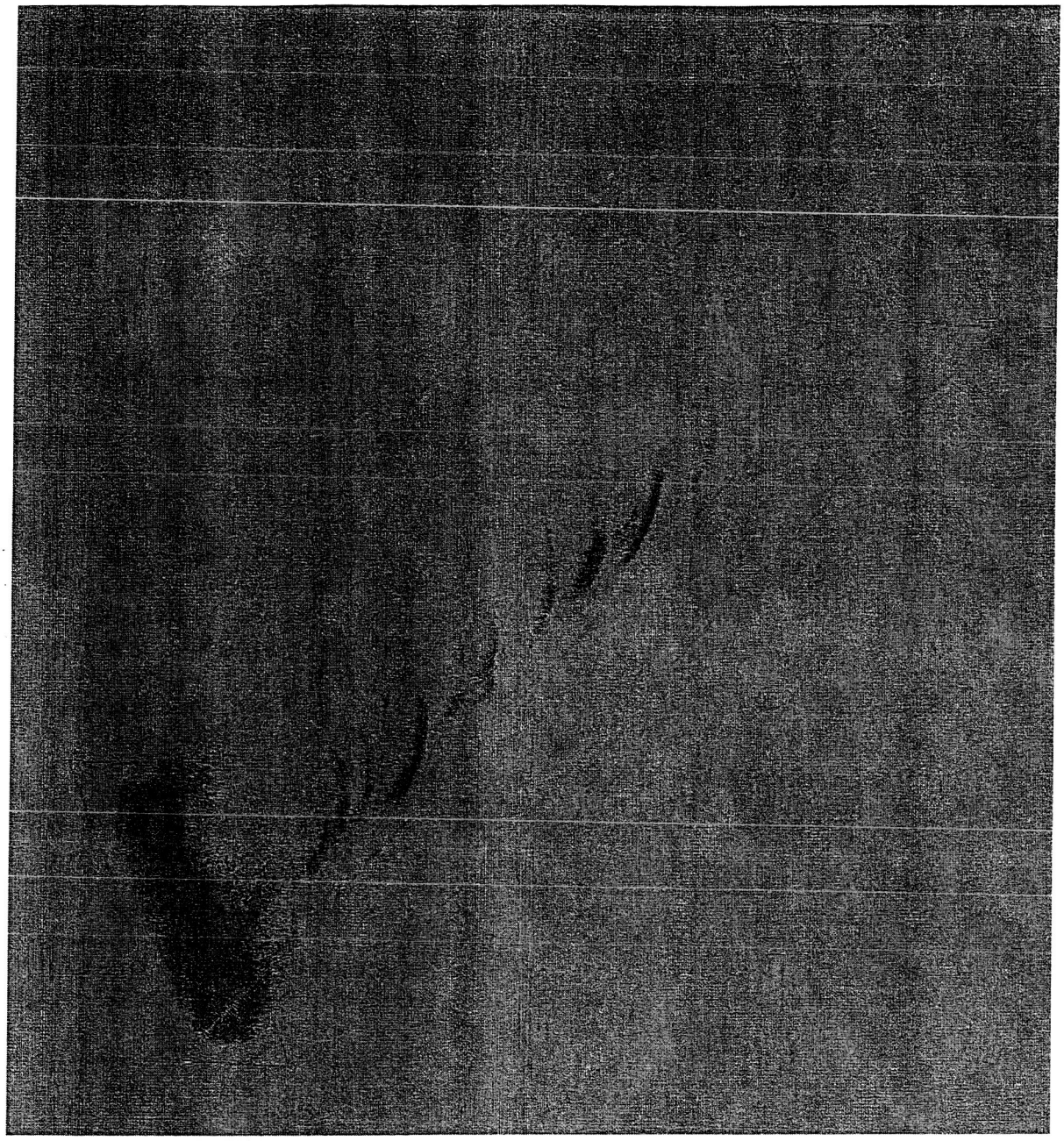

Figure 16. Isometric view of lead wire trace in FSW sample. Note the aluminum matrix has been subtracted from view.

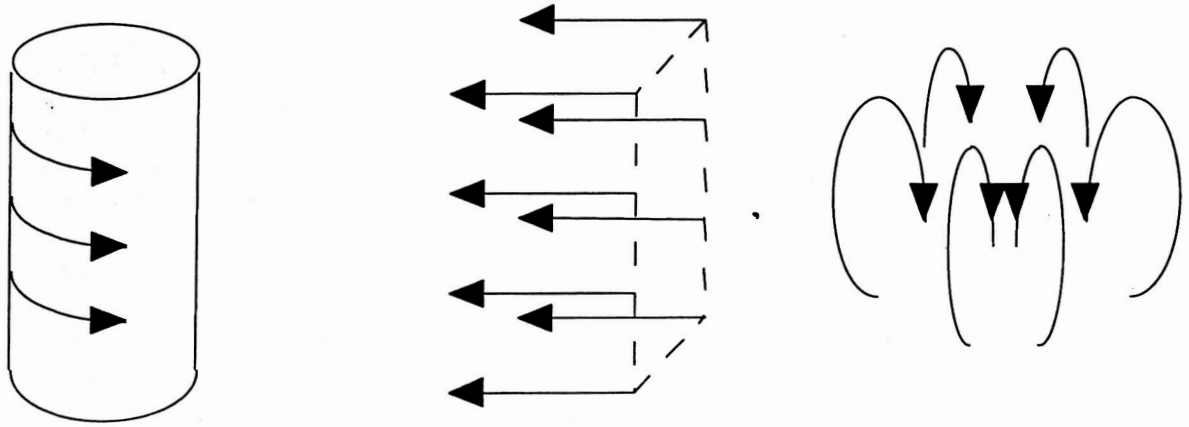

Figure 17. Three incompressible flow fields of the friction stir weld: a) rigid body rotation, b) uniform translation, and c) ring vortex.